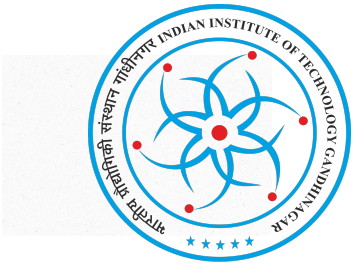

Tilted Mott Insulator in an Optical Cavity

Ashesh Kumar Gupta

Master Thesis in Physics
Department of Physics
Indian Institute of Physics Gandhinagar

Supervisor Prof. B Prasanna Venkatesh

25th April 2024

Abstract

In this work we seek to expand the study of the quantum phases of a tilted Mott insulator pioneered in [9] to the case of an intra-cavity Mott insulator (MI) studied in some detail first in [4]. The ultimate aim is two-fold: understand the phases and phase transitions of a tilted intra-cavity MI and explore whether this system can be used to propose a quantum phase transitions enhanced highly sensitive read-out of the force/tilt.

The famed Bose-Hubbard model at $T = 0$ (eq. 1.2 in [9] with $E = 0$), there is a quantum phase transition from superfluid (long range coherent state with $\hat{b}_i \neq 0$) to a Mott insulator as w/U is decreased. In [9], starting with such Mott Insulator phases, they show that adding a uniform field E leads to another interesting quantum phase transition at $E = U$ where the parent Mott Insulator state is resonantly coupled to states with dipole excitations. We want to extend this study to the case of an intracavity MI first considered in [4]. Here, the periodic potential is provided by the intracavity standing wave and the atomic state is coupled to the field dynamics. Thus, the atomic state has to be self-consistently solved with the field state. This leads to very interesting phase diagram for the MI-SF transition in the cavity case different from the one for the usual MI-SF in a free-space optical lattice.

Acknowledgements

I would like to express my gratitude to my supervisor,Prof. B Prasanna Venkatesh, for teaching and inspiring me in my MSc studies.

Contents

1 Quantum Phase Transitions

Phase transitions are fundamental in natural phenomena, manifesting in everyday occurrences like water boiling or ice melting. More complex transitions include metals transitioning into superconducting states as temperatures decrease. These transitions occur due to changes in external parameters, leading to qualitative shifts in system properties. While many transitions occur at finite temperatures, where thermal fluctuations disrupt macroscopic order (e.g., crystal structures during melting), recent attention has focused on zero-temperature phase transitions. Here, non-thermal parameters like pressure, magnetic fields, or chemical compositions are adjusted to reach transition points, where quantum fluctuations—arising from the Heisenberg uncertainty principle—destroy order.

Quantum phase transitions(QPT) have become a vibrant study area in contemporary condensed matter physics. Initially perceived as niche topics concerning special points on phase diagrams reachable only at absolute zero temperature, recent experimental and theoretical advancements have shown the broader significance of these transitions. These transitions offer crucial insights into the emergence of novel finite-temperature states of matter near their critical points. Unlike conventional phase transitions influenced by thermal fluctuations, QPTs occur at absolute zero temperature and are driven solely by quantum fluctuations. Critical points in the parameter space, marked by non-analyticities in the ground state energy density, define these QPTs. At these critical points, one observes the length divergence associated with the two-point correlation function of relevant quantum fields. Another characteristic of QPTs is the vanishing energy gap between the ground and the first excited state in the thermodynamic limit at critical points. These features collectively characterise the unique nature of quantum phase transitions and their significance in understanding the complex behaviours of matter under extreme conditions.

In systems near a continuous phase transition, such transitions are typically characterised by an order parameter. This parameter is a thermodynamic quantity that remains zero in one phase (the disordered phase) and becomes non-zero and non-unique in the other phase (the ordered phase). Often, selecting an order parameter for a specific transition is straightforward, such as in the case of the ferromagnetic transition, where the total magnetisation serves as the order parameter. In our case, however, determining an appropriate order parameter can be complex.

The importance of quantum mechanics in understanding continuous phase transitions has two main aspects. Firstly, in some cases, quantum mechanics is crucial for explaining the existence of ordered phases, such as in superconductivity, depending on the specific transition

under consideration. Secondly, there's a question of whether quantum mechanics influences the asymptotic critical behavior of the system.

To address this, we compare two energy scales: $\hbar\omega_c$, representing the typical energy of long-distance order parameter fluctuations, and the thermal energy k_BT. As a continuous transition is approached, the typical time scale τ_c of fluctuations diverges, leading to the typical frequency scale ω_c approaching zero, and consequently, the typical energy scale $\hbar\omega_c = |t|^{\nu z}$.

Quantum mechanics remains significant as long as $\hbar\omega_c$ is larger than k_BT. In contrast, when $\hbar\omega_c$ becomes much smaller than k_BT, a purely classical description suffices for order parameter fluctuations. This transition from quantum to classical behavior occurs when $\hbar\omega_c$ falls below k_BT.

For transitions occurring at finite temperatures T_c, quantum mechanics becomes negligible for $|t| < T_c^{1/\nu z}$, implying that the critical behaviour near the transition is entirely classical. This categorises all finite-temperature phase transitions as "classical," where classical thermal fluctuations dominate macroscopic scales controlling critical behaviour. However, transitions occurring at zero temperature with respect to a non-thermal parameter r, like pressure or magnetic field, are always dominated by quantum fluctuations, earning them the label of "quantum" phase transitions.

1.1 FIDELITY SUSCEPTIBILITY AS A MEASURE FOR QPT

Fidelity and Berry phase have also been used to analyse quantum phase transitions from a geometrical perspective recently. Fidelity, in particular, offers a unique perspective as it is a spatial geometric quantity. Unlike traditional methods that rely on prior knowledge of the order parameter and symmetry breaking, fidelity-based studies of quantum phase transitions require no such assumptions. This makes fidelity a powerful tool for investigating the underlying geometrical structures associated with quantum phase transitions, offering insights that complement and enhance our understanding of these complex phenomena.

The spectra reconstruction process for a general quantum system is governed by the Hamiltonian:

$$H(\lambda) = H_0 + \lambda H_1, \tag{1.1}$$

where the eigenvalue equation is given by:

$$H(\lambda)|\Psi_n(\lambda)\rangle = E_n|\Psi_n(\lambda)\rangle \tag{1.2}$$

Fidelity susceptibility (χ_F) offers a geometric approach to studying QPTs. It is based on the fidelity,

$$F_i(\lambda, \delta) = |\langle\Psi_0(\lambda)|\Psi_0(\lambda + \delta)\rangle|$$

, which measures the overlap between ground states for nearby values of the control parameter λ. The key expressions for fidelity susceptibility are:

$$\frac{1}{F_i^2} = 1 + \delta\lambda^2 \sum_{n\neq 0} \frac{|\langle\Psi_n(\lambda)|H_1|\Psi_0(\lambda)\rangle|^2}{[E_n(\lambda) - E_0(\lambda)]^2} \tag{1.3}$$

$$\chi_F(\lambda) = \sum_{n\neq 0} \frac{|\langle\Psi_n(\lambda)|H_1|\Psi_0(\lambda)\rangle|^2}{[E_n(\lambda) - E_0(\lambda)]^2} \tag{1.4}$$

$$\chi_F = \lim_{\delta\lambda\to 0} \frac{-2\ln F_t}{\delta\lambda^2} \tag{1.5}$$

χ_F exhibits divergences at quantum critical points, making it a useful indicator of phase transitions. The scaling behavior of χ_F near the critical point can provide information about the universality class of the QPT. In ultracold atomic gases, χ_F has been measured through interferometric techniques that probe the overlap between ground states.

2

Bose-Hubbard Model

In this chapter, we focus on the Bose-Hubbard model, which describes a Bose gas in an optical lattice. As initially explored by [1], it will be demonstrated that this model has a quantum phase of matter known as the Mott-Insulator phase. Furthermore, as a function of the interaction potential, it is projected that the Bose gas will experience a quantum phase transition from the superfluid state to the Mott-insulator state. The observation of this quantum phase transition in a groundbreaking experiment by [2] has garnered significant interest. It demonstrated the possibility of stimulating several lattice models of vital importance to condensed matter physics using ultracold atoms in an optical lattice.

The phase diagramm of the model is derived using a mean-field approach combined with the non-degenerate pertubation theory. It will be looked closely at the effects that lead to the transition and at the peculiarities of the phase boundary itself.

The Hamiltonian for the Bose-Hubbard Model in the second quantized form is given by

$$H = -t \sum_{<i,j>} a_i^\dagger a_j - \sum_i (\epsilon_i - \mu) a_i^\dagger a_i + \frac{U}{2} \sum_i a_i^\dagger a_i^\dagger a_i a_i \tag{2.1}$$

or using the commutation relation for bsosons, $[a_i, a_j^\dagger] = \delta_{i,j}$, this can be written equivalently as

$$H = -t \sum_{<i,j>} a_i^\dagger a_j - \sum_i (\epsilon_i - \mu) \hat{n}_i + \frac{U}{2} \sum_i \hat{n}_i (\hat{n}_i - 1) \tag{2.2}$$

where $\hat{n}_i = a_i^\dagger a_i$ is the occupation number on site i. This is the model that will be analyzed in this thesis. In the following discussion the on-site energy ϵ_i will be assumed to be the same on all sites and therefore set to zero for simplicity. This may be done because it simply gives an energy offset on every site.

2.1 PHASE TRANSITION IN BOSE- HUBBARD MODEL

The Bose-Hubbard model describes a Mott-insulator-Superfluid transition. This model is described by the Hamiltonian Eq.(2.2) but with $\epsilon = 0$.

$$H = -t \sum_{<i,j>} a_i^\dagger a_j - \mu \sum_i \hat{n}_i + \frac{U}{2} \sum_i \hat{n}_i (\hat{n}_i - 1) \tag{2.3}$$

With $U > 0$, repulsive on-site interaction and μ, the chemical potential, which fixes the particle number. The chemical potential μ is the "tilt" between these two bowls of particles, allowing for particles to flow until equilibrium (same number of particles, fixed desired N) is reached.

The creation and annihilation operators $a_i^\dagger$ and a_i satisfies the commutator relation $[a_i, a_j^\dagger] = \delta_{i,j}$ and hence describe spinless bosonic particles.The term, $\hat{n}_i = a_i^\dagger a_i$ is the occupation number operator for lattice site i. The first term of the Hamiltonian describes the dynamics of the system: a_j destroys one particle on the site j and $a_i^\dagger$creates one on another site i, where the sites i, j are the next nearest neighbors ($< i, j >$ represents nearest neighbor pairs). 't' is the hopping amplitude, which governs this process. The third term (interaction term) describes the on-site repulsion of two or more particles at the same lattice site. For the case when none or one particle at the same site there is no interaction.

By considering the cases where $t/U \to 0$ and $U/t \to 0$ we would see that the system is in completely different phases for the two possibilities. Assuming that there is only one boson on average ($\bar{n} = 1$), in the limit of $t/U \to 0$, then there must be one boson on each lattice site. Moving a particle would create an empty and a doubly-occupied lattice site which would require a very large energy (U) with respect to the gain in kinetic energy(t). Hence, the chances of this happening is very little. Therefore, for an specific density of particles, the bosons will be suppressed to move from one site to another and the system is in an insulating state. Whereas in the opposite limit when $U/t \to 0$, the system becomes superfluid. In this state, the particles can move without resistance through the system. Thus, as the ratio t/U increases we expect a phase transition between an insulating ground state (known as a Mott-insulating phase) and a superfluid ground state. As it appears only at T = 0, it is called a quantum phase transition[8]. In the usual case the phase transition is driven by thermal fluctuations. That is not possible for T = 0, the fluctuations are of quantum nature. They appear because of the Heisenberg uncertainty principle and become so strong that phase transitions can happen. Therefore, they are called quantum phase transitions.

2.2 MOTT-INSULATING PHASE

First, it will be considered the strong coupling limit without hopping $t = 0$ and $U >> 1$. The Hamiltonian becomes

$$H_{t=0} = \sum_{i=1}^{M} \left(\frac{U}{2} \hat{n}_i (\hat{n}_i - 1) - \mu \hat{n}_i \right) \tag{2.4}$$

where M is the number of lattice sites. This Hamiltonian is local and therefore the same on all lattice sites. Hence, on can focus on the local Hamiltonian

$$H_{loc} = \left(\frac{U}{2} \hat{n}(\hat{n} - 1) - \mu \hat{n} \right) \tag{2.5}$$

which is diagonal in the occupation number state $|n\rangle$. This follows from the fact that H_{loc} commutes with $\hat{n}$.

Computing the eigenvalues of H_{loc} in its eigenbase, one obtains

$$\epsilon_n : \langle n|H_{loc}|n\rangle = \frac{U}{2}n(n-1) - \mu n \tag{2.6}$$

So, to find the occupation n_0, which minimizes the energy of the ground state,

The ground state $|n_0\rangle$ is defined as the eigenstate of $\epsilon_{n_0} = min_n\epsilon_n$, where the number n can only be an integer or zero. The most stable state is when there is the same number of particles on all sites. It is known that the ground state is a Mott-insulator. By calculating the energy cost to add or remove one particle to the system, we can find the values of n_0. Assuming ϵ_{n_0} is the ground state, then the energy cost to add one particle to the system is,

$$\epsilon_{n_0} < \epsilon_{n_0} + 1 = \frac{U}{2}n_0(n_0+1) - \mu(n_0+1) = \epsilon_{n_0} + Un_0 - \mu$$

The condition for $n_0 > \frac{\mu}{U}$ is given by the above equation. Also, the cost to remove a particle,

$$\epsilon_{n_0} < \epsilon_{n_0} - 1 = \frac{U}{2}(n_0-1)(n_0-2) - \mu n_0 = \epsilon_{n_0} + U(1-n_0) - \mu$$

and from this relation follows $\frac{\mu}{U} > n_0 - 1$. Summarizing both the conditions, we can find the dependence of n_0 on $\frac{\mu}{U}$,

$$n_0 > \frac{\mu}{U} > n_0 - 1 \tag{2.7}$$

If initially there was no particle in the state $(n_0 = 0)$, one only has the condition $\mu/U < n_0 = 0$. Hence, the occupation number in the ground state depending on μ/U is

$$n_0 = \begin{cases} 0 & \text{for } \mu/U < 0 \\ 1 & \text{for } 0 < \mu/U < 1 \\ 2 & \text{for } 1 < \mu/U < 2 \\ \vdots & \\ n & \text{for } n-1 < \mu/U < n \end{cases} \tag{2.8}$$

Also, by asking what energy is needed to excite one boson from one site to another, which leaves a site with occupancy $n-1$ and creates one with $n+1$, leads to the so-called excitation gap of the Mott insulator.

A non-vanishing excitation gap is a characteristic property of the insulating phase. The excitation gap for t = 0 is the sum of the energy cost needed to add and to remove one particle from the system and will be denoted as Δ_0

$$\Delta_0 = \epsilon_{n_0+1} - \epsilon_{n_0} = U \tag{2.9}$$

The excitation spectrum of the superfluid phase is gapless.

Also, the states where μ/U takes an integer value are doubly degenerate on every site. This degeneracy will be lifted by a non-zero t. We can derive the ground state of the insulating phase by a variational ansatz for this state which minimizes the expectation value of the Hamiltonian $H_{t=0}$ and which is normalized. The ground state is[6]

$$|\Omega\rangle = \prod_{i=1}^{M} \frac{1}{\sqrt{n_0}} (a_i^\dagger)^{n_0} |0\rangle \tag{2.10}$$

The ground state is just a Fock state with the same number of particles n_0 (occupancy for minimal energy) on each site of the lattice.

2.3 SUPERFLUID PHASE

For the limit $U/t << 1$ one can set $U = 0$ for simplicity. The Hamiltonian then becomes

$$H_{U=0} = -t \sum_{<i,j>} a_i^\dagger a_j - \mu \sum_i a_i^\dagger a_i \tag{2.11}$$

This Hamiltonian can be diagonalized by Fourier transforming the apperaring creation and annihilation operators [6].

$$\begin{aligned} a_j &= \frac{1}{\sqrt{N}} \sum_{\vec{k}} e^{i\vec{k}\cdot\vec{R}_j} a_{\vec{k}} \\ a_j^\dagger &= \frac{1}{\sqrt{N}} \sum_{\vec{k}} e^{-i\vec{k}\cdot\vec{R}_j} a_{\vec{k}}^\dagger \end{aligned} \tag{2.12}$$

Inserting them into $H_{U=0}$, we get,

$$H_{U=0} = \sum_{\vec{k}} (\epsilon_{\vec{K}} - \mu) a_{\vec{k}}^\dagger a_{\vec{k}} \tag{2.13}$$

with $\epsilon_{\vec{k}} = -2t \sum_{a=1,2,\cdots d} \cos(ka)$ where e the lattice spacing a between neighboring lattice sites was set to one. The resulting Hamiltonian in this limit describes a free Bose gas. The free Bose gas provides the simplest realization of a free Bose-Einstein condensation. The Bose-Einstein condensate is a state of matter that bosonic systems can reach under a critical tempereture. The statistic of bosons allows an arbitrary number of particles to be in a quantum state. For small temperatures the particles tend to be in the state with the lowest energy. Hence, due to the statistic the majority of the bosons will be in the state of lowest energy for a sufficiently small temperature.

In the present case where T = 0 all the bosons will occupy the state where $\vec{k} = 0$ which is obviously the one with the lowest energy. The ground-state ket of the system for a fixed particle number N is, however

$$|\Omega\rangle = \left(\frac{1}{\sqrt{N}} \sum_{i=1}^{M} a_i^\dagger \right)^N |0\rangle \tag{2.14}$$

This means that all bosons are maximally delocalized with probability $\approx 1/N$ to be found on an arbitrary lattice site. So the wavefunction of every boson is spread over the whole lattice

which indicates the superfluid state where all bosons can move freely over the whole lattice. This gound state holds in canonical ensemble where the number of particles is fixed at N.

If we fix the average densiy of particles on the lattice at $< a_i^\dagger a_i >= \frac{N}{M} = n$, then we get the ground state as,

$$|\Omega\rangle = \prod_{i=1}^{M} \left(e^{\sqrt{N/M} a_i^\dagger} \right) |0\rangle \tag{2.15}$$

This is a product of coherent states at each lattice site, which has the same intepretation as the ground-state in the canonical state. The expectation value $< a_i >$ is the order parameter of the superfluid state. The non-vanishing of this order parameter indicates that the sytem is in a suerfluid state.

2.4 MEAN FIELD THEORY

It is not possible to find a transition from the superfluid to the Mott-insulating state, known from the Bogoljubov theory for a weakly interacting bosonic gas. This theory would describe the transition between a normal gas and the superfluid state[10]. One has to start from the other limit, i.e. the transistion from the Mott-insulating state to the superfluid state.

Let's suppose the model is in initially Mott-insulating state and taking the hopping amplitude t > 0 and perform a mean field decoupling in the hopping term of the Hamiltonian Eq.(2.3).

So, let's with the hamiltonian,

$$H = -t \sum_{<i,j>} a_i^\dagger a_j - \mu \sum_i \hat{n}_i + \frac{U}{2} \sum_i \hat{n}_i(\hat{n}_i - 1)$$

and decouple the hopping term by assuming that the expectation value $< a_i > \equiv \phi$, is non-zero but small and the same on all sites. ϕ is in analogy the Bogoljubov theory the order parameter of the superfluid state. Expand the creation and annihilation operator in the hopping term around their expectation values plus small fluctuations $a_i = \phi + \delta a_i$, so that the product $a_i^\dagger a_j$ can be written as

$$a_i^\dagger a_j = \phi a_i^\dagger + \bar{\phi} a_j - |\phi|^2$$

In this approximation, the hamiltonian becomes,

$$H_{MF} = \left(-\mu \sum_i \hat{n}_i + \frac{U}{2} \sum_i \hat{n}_i(\hat{n}_i - 1) \right) - t \sum_{<i,j>} \left(\phi a_i^\dagger + \bar{\phi} a_j - |\phi|^2 \right) \tag{2.16}$$

$$H_{MF} = \left(-\mu \sum_i \hat{n}_i + \frac{U}{2} \sum_i \hat{n}_i(\hat{n}_i - 1) + tz|\phi|^2 \right) - tz \sum_i \left(\phi a_i^\dagger + \bar{\phi} a_j \right) \tag{2.17}$$

where z is the coordination number, counting the number of next nearest neighbors. The MF Hamiltonian is now an local Hamiltonian.

$$H_{loc} = h + V^t \tag{2.18}$$

The eigenstates of the unperturbed Hamiltonian $\sum_i h$ are the same as previous

$$|\Omega\rangle = \prod_{i=1}^{M} \frac{1}{\sqrt{n_0}} (a_i^\dagger)^{n_0} |0\rangle \tag{2.19}$$

but with the eigenvalues,

$$E_{n_0} = \frac{U}{2} n_0(n_0 - 1) - \mu n_0 + tz|\phi|^2 \tag{2.20}$$

The occupation number is also same as before given in Eq.(2.8).

To calculate the energy and energystate corrections, we need to compute using perturbation theory. Correction to the p-th order,

$$E_n^{(p)} = \langle n_0^{(0)} | V^t | n_0^{p-1} \rangle \tag{2.21}$$

with $|n_0\rangle = \frac{1}{\sqrt{n_0}} (a_i^\dagger)^{n_0} |0\rangle$. Due to the fact that the pertubation V^t is linear in the creation and annihilation operator, all corrections of an odd order to the the energy will vanish in the occupation number basis. Therefore, the first order correction will vanish,

$$E_n^{(1)} = \langle n_0 | V^t | n_0 \rangle = 0 \tag{2.22}$$

And the state- correction,

$$\begin{aligned}
|n_0^{(1)}\rangle &= \sum_{m \neq n} |m_0\rangle \frac{\langle m_0| - tz(\phi a^\dagger + \bar{\phi} a)|n_0\rangle}{E_{n_0}^0 - E_{m_0}^0} - E_{n_0}^{(1)} \sum_{m \neq n} |m_0\rangle \frac{\delta_{n_0}\delta_{m_0}}{E_{n_0}^0 - E_{m_0}^0} \\
&= \sum_{m \neq n} |m_0\rangle \frac{-tz(\phi\sqrt{n_0+1}\delta_{m_0}\delta_{n_0+1} + \bar{\phi}\sqrt{n_0}\delta_{m_0}\delta_{n_0-1})}{E_{n_0}^0 - E_{m_0}^0} \\
&= -tz \left[\frac{(\phi\sqrt{n_0+1}|n_0+1\rangle}{E_{n_0}^0 - E_{n_0+1}^0} + \frac{\bar{\phi}\sqrt{n_0}|n_0-1\rangle}{E_{n_0}^0 - E_{n_0-1}^0} \right] \\
&= -tz \left[\frac{(\phi\sqrt{n_0+1}|n_0+1\rangle}{\mu - Un_0} + \frac{\bar{\phi}\sqrt{n_0}|n_0-1\rangle}{U(n_0-1) - \mu} \right]
\end{aligned} \tag{2.23}$$

Now, with this result, we get the second order correction,

$$\begin{aligned}
E_{n_0}^{(2)} = \langle n_0 | V^t | n_0^{(1)} \rangle &= (tz)^2 \left[\langle m_0| - tz(\phi a^\dagger + \bar{\phi} a) \left(\frac{(\phi\sqrt{n_0+1}|n_0+1\rangle}{\mu - Un_0} + \frac{\bar{\phi}\sqrt{n_0}|n_0-1\rangle}{U(n_0-1) - \mu} \right) \right] \\
&= (tz)^2 \left[\frac{n_0+1}{\mu - Un_0} + \frac{n_0}{U(n_0-1) - \mu} \right] |\phi|^2
\end{aligned} \tag{2.24}$$

The Landau theory of phase transitions can be used to argue where the phase transition appear.

$$E_0 = a_0 + a_2|\phi|^2 + a_4|\phi|^4 + O(|\phi|^6) \tag{2.25}$$

with

$$\begin{aligned} a_0 &= \frac{U}{2} n_0(n_0-1) - \mu n_0 \\ a_2 &= tz + (tz)^2 \left[\frac{n_0+1}{\mu - U n_0} + \frac{n_0}{U(n_0-1)-\mu} \right] \end{aligned} \tag{2.26}$$

According to Laudau theory, the phase transition happens when, a_2 vanishes if a_4 is positive, which it is,

$$\frac{\partial E}{\partial \bar{\phi}} = a_2 \phi + 2a_4 |\phi|^2 \phi = 0 \tag{2.27}$$

or,

$$\phi_0 = 0, \text{or}, |\phi_\pm| = \frac{-a_2}{2a_4}$$

The solution that minimizes the energy is the one for which the second derivative is positive. This will depend on the sign of a_2.

$$\frac{\partial^2 E}{\partial \phi \partial \bar{\phi}} = a_2 + 4a_4 |\phi|^2 > 0 \tag{2.28}$$

$$|\phi| = \begin{cases} 0 & \text{for } a_2 > 0 \\ \sqrt{\frac{-a_2}{4a_4}} & \text{for } a_2 < 0 \end{cases} \tag{2.29}$$

Due to the fact that the order parameter ϕ is non-zero for $a_2 < 0$ and zero for $a_2 > 0$, there has to be a phase transition of second order for $a_2 = 0$. The order parameter ϕ characterizes the superfluid phase. If $|\phi| = 0$, then the hopping term will be zero, so for $a_2 > 0$, the system will be in a Mott-insulator phase, and for $a_2 < 0$, it will be in a superfluid phase. Now, at $a_2 = 0$,

$$a_2 = tz + (tz)^2 \left[\frac{n_0+1}{\mu - U n_0} + \frac{n_0}{U(n_0-1)-\mu} \right] = 0 \tag{2.30}$$

Defining, $\bar{\mu} = \mu/U$ and $w = tz/U$ and solving for w, we get,

$$w = \frac{(n_0 - \bar{\mu})(\bar{\mu} - (n_0 - 1))}{\bar{\mu} + 1} \tag{2.31}$$

At $w = 0$, the the Superfluid-Mott-insulator transition appears. Going back to the cases where the ground state energy of the system is degenerate, $\mu = U n_0$ or $\mu = U(n_0 - 1)$. Solving for $\bar{\mu}$, we get,

$$\bar{\mu}^2 - \bar{\mu}(2n_0 - 1 - w) + w + n_0(n_0 - 1) = 0 \tag{2.32}$$

$$\bar{\mu} = n_0 - 1/2 - w/2 \pm \sqrt{w^2 - 4w(n_0 + 1/2) + 1} \tag{2.33}$$

For $\bar{\mu}$ to be real, we need $\sqrt{w^2 - 4w(n_0 + 1/2) + 1} > 0$, or,

$$w_c = 2n_0 + 1 - 2\sqrt{n_0(n_0+1)} \tag{2.34}$$

and

$$\bar{\mu} = -1 + \sqrt{n_0(n_0+1)} \tag{2.35}$$

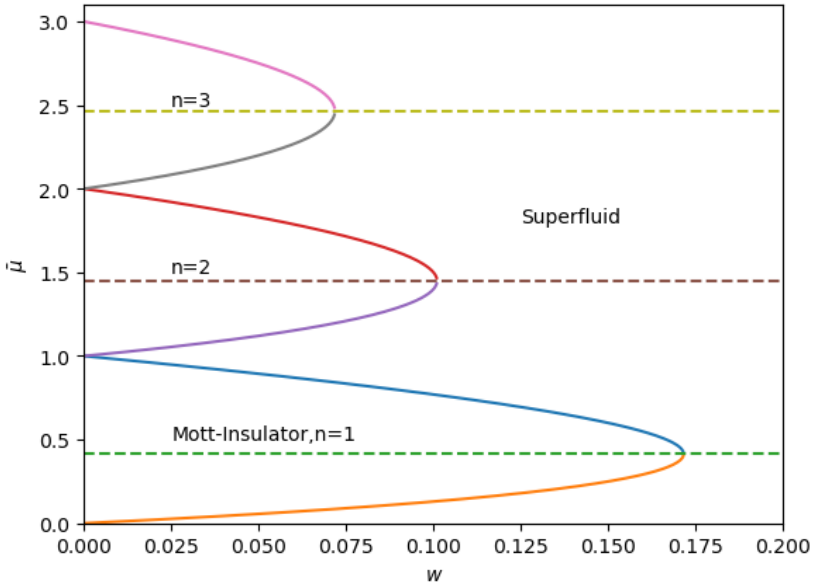

Figure 2.1: Mean-field phase diagram of the Bose-Hubbard model showing the first three Mott-lobes and the superfluid phase.

3

Tilted Double-Well

The single-level Bose-Hubbard Hamiltonian for N atoms in a double-well system is given by:

$$H = -J(\hat{a}_L^\dagger \hat{a}_R + \hat{a}_R^\dagger \hat{a}_L) + U[\hat{n}_L(\hat{n}_L - 1) + \hat{n}_R(\hat{n}_R - 1)] - \epsilon(\hat{n}_L - \hat{n}_R) \tag{3.1}$$

Here, $\hat{a}_i^\dagger$ ($\hat{a}_i$) creates (annihilates) a boson in the i-th well (i = L, R), $\hat{n}_i = \hat{a}_i^\dagger \hat{a}_i$ represents the number operator for the i-th well, J is the tunneling energy, and U is the on-site interaction (where a positive U corresponds to attractive atom-atom interaction). V0 is the tilt parameter, which breaks the left-right symmetry and is typically nonzero in experimental setups. For convenience, we set J = 1 and focus on U > 0 in this discussion.

This Hamiltonian can be diagonalized in the (N + 1)-dimensional Fock space spanned by $|n_L, n_R\rangle = |N - n_L\rangle$, where n_L and n_R represent the number of atoms in the left and right wells, respectively. The dynamics of the system are governed by the parameter $\lambda \equiv N\frac{U}{J}$. As λ transitions from the weak region to the fermionization limit, the behavior of these atoms, initially mostly confined to one well, evolves from Josephson oscillations (simple tunneling between wells) to self-trapping above a critical interaction strength.

The ground state properties of the Bose-Hubbard Hamiltonian (Equation (3.1)) are significantly influenced by the ratio of local interaction energy to tunneling coupling, $\frac{U}{J}$. In the strong interaction regime, the ground state is localized in the atom number basis with low coherence when U/J is large, while strong coupling leads to high coherence and a delocalized state.

Fig. 3.2 illustrates the distribution of atom number states and ensemble-averaged momentum distributions for three U/J ratios. As U/J increases, atom number fluctuations vanish before coherence decreases, defining three regimes[7] :

1. Rabi regime: $U/J < 10^{-4}$ where coherence is very high with large atom number fluctuations, akin to the non-interacting limit.

2. Josephson regime: $10^{-4} < U/J < 1$ with reduced atom number fluctuations but high coherence, allowing for a relative phase definition.

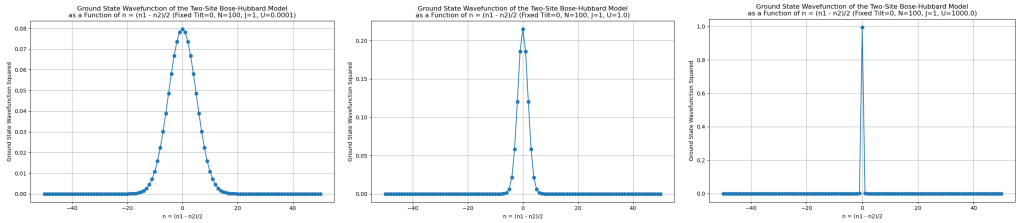

(a) Rabi Regime (b) Josephson Regime (c) Fock Regime

Figure 3.1: The distribution of atom number states for three different ratios of U/J without tilt

3. Fock regime: $U/J > 1$ dominated by interaction energy, leading to well-defined atom numbers per well and complete phase uncertainty due to vanished coherence.

In the Rabi regime, the system behaves as N-independent particles with Poissonian atom number states and high coherence. The Josephson regime exhibits reduced fluctuations and high coherence, supporting a relative phase definition. Large atom numbers in this regime may enable mean-field descriptions. The Fock regime is characterized by well-defined atom numbers and no coherence, rendering the phase undefined in the Josephson junction.

Now, we will add tilt into the system and see how it effects the system,

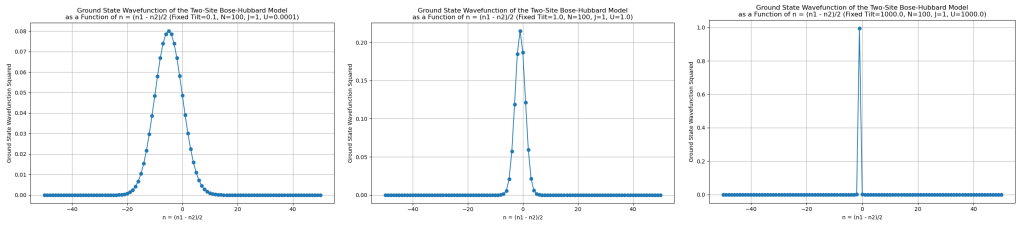

(a) Rabi Regime (b) Josephson Regime (c) Fock Regime

Figure 3.2: The distribution of atom number states for three different ratios of U/J with tilt

Now, to understand the phase transition due to tilt, we will study the Fidelity Susceptibility of the system. In Fig. 1, we fix the particle number N to show the relation between $\chi(\lambda)$ and epsilon. With the increase of epsilon, the peak moves towards right. The behavior of $\chi(\lambda)$ can be understood through the analysis of the ground state, which can be expanded as $|\Psi_0\rangle = \sum_{k=0}^{N} c_k |k, N-k\rangle$, where $n_L = k$ and $n_R = N - k$.

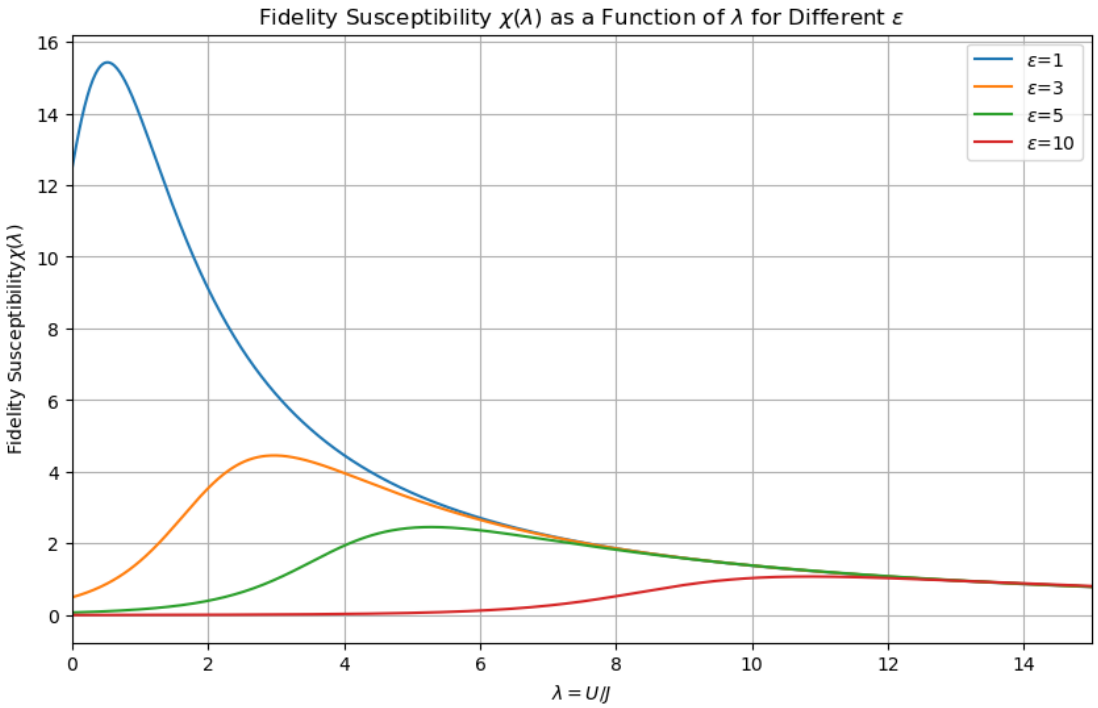

Figure 3.3: he fidelity susceptibility $\chi(\lambda)$ for N = 100 under tilt $\epsilon = 1, 3, 5, 10$. One can see a that the phase transition occurs at $U = \epsilon$

As we can see in Fig. 3.3 we get the fidelity peak at $U = \epsilon$, so, we get a phase transition point at the critical point, $U_c = \epsilon$, the tilt point.

So far our discussion is based on a fixed particle number N . Now we need to fix the tilt and enlarge N to see what happens in the large-N limit. As we can see in Fig. 3.4, the fidelity value increases with N. Now, we can see that, phase transition points still remain the same $U_c = \epsilon$.

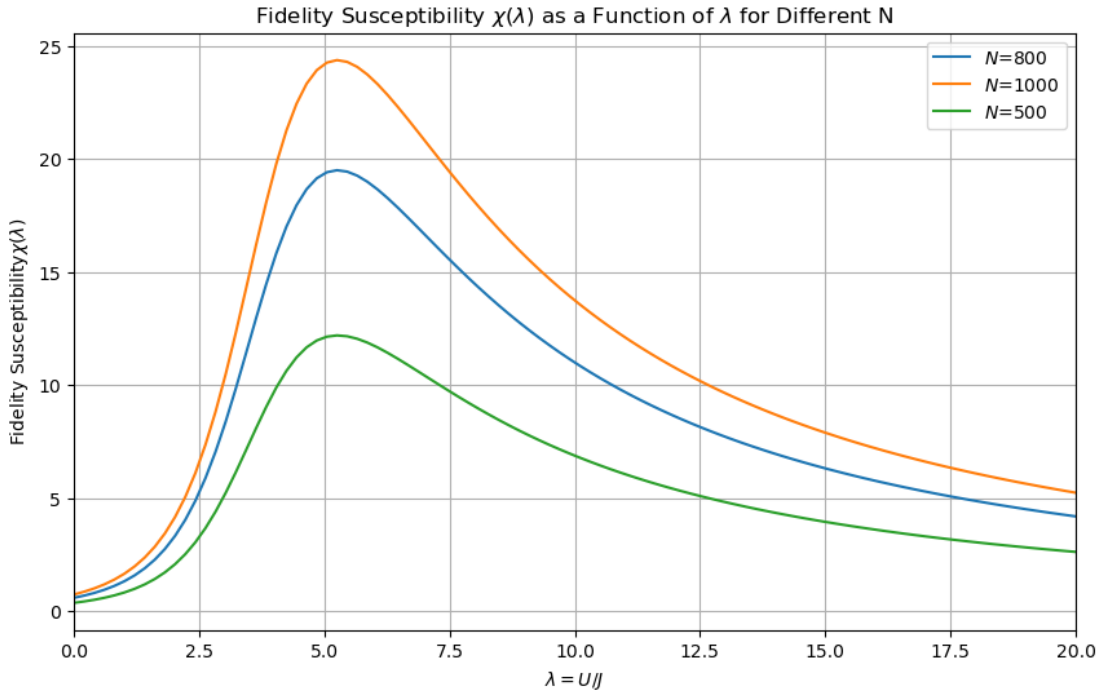

Figure 3.4: The fidelity susceptibility $\chi(\lambda)$ under tilt $\epsilon = 5$ for different N. One can see a that the fidelity value increases with N

4

Tilted Mott Insulator Phase Transition

In [9], they studied a Mott-insulating state of ^{87}Rb atoms, which is s stable to a small applied potential gradient (an 'electric' field), but a resonant response was observed when the potential energy drop per lattice spacing (E), was close to the repulsive interaction energy (U) between two atoms in the same lattice potential well. They identified all states which are resonantly coupled to the Mott insulator for $E \approx U$ via an infinitesimal tunneling amplitude between neighboring potential wells. The strong correlation between these states is described by an effective Hamiltonian for the resonant subspace. This Hamiltonian exhibits quantum phase transitions associated with an Ising density wave order, and with the appearance of superfluidity in the directions transverse to the electric field.

The modified Bose-Hubbard Model in presence of the electric field is given by,

$$H = -w \sum_{<i,j>} (b_i^\dagger b_j + b_j^\dagger b_i) + \frac{U}{2} \sum_i n_i(n_i - 1) - E \sum_i e \cdot r_i n_i \tag{4.1}$$

r_i are the spatial co-ordinates of the lattice sites (the lattice spacing is unity), and e is a vector in the direction of the applied electric field (e is not necessarily a unit vector—its length is determined by the strength of the electric field).

Now, when E = 0, the system is in a Mott insulator with n_0 particles per site. Now, when $E \approx U$, the system starts to change. For, $w << U$, and for most values of E, the experiments displayed little detectable change in the state of the system. This is because with large U, the motion of the particle will be along the direction of e, just the hopping term will be replaced by $w(n_0 + 1)$, so any such states created above the Mott insulator will remain localized and will not have the chance to extend across the system to create large changes in the initial state. It is just a deformation of the Mott state which carries a net charge. Now, [2], shows that when such a state does not carry any net charge, an important neutral deformation of the Mott state—it is the dipole state consisting of a quasiparticle-quasihole pair on nearest neighbor sites. Only their paired motions will be important along e, let's call them dipole states.

For $w = 0$, such states are diagonal in the number state basis like in Eq.(2.5),

$$H_{loc} = \frac{U}{2} \sum_i n_i(n_i - 1) - E \sum_i e \cdot r_i n_i \tag{4.2}$$

$$\epsilon_n = \frac{U}{2} n(n - 1) - E \sum_i e \cdot r_i n \tag{4.3}$$

Now, again like in the sec(1.2), the ground state would when there are same number of particles at all sites. And the energy cost to add or remove a particle from a site is bounded by,

$$n_0 > E/U > n_0 - 1 \tag{4.4}$$

Also, the energy required to remove a particle from site i,

$$\begin{aligned}[\epsilon_{n_o-1} - \epsilon_{n_0}]_i &= \frac{U}{2}(n_0-2)(n_0-1) - E\sum_i e\cdot r_i(n_0-1) - \frac{U}{2}(n_0)(n_0-1) + E\sum_i e\cdot r_i(n_0) \\ &= U(1-n_0) + E\sum_i e\cdot r_i\end{aligned} \tag{4.5}$$

And, the energy required to add a particle from the site (i+1),

$$\begin{aligned}[\epsilon_{n_o+1} - \epsilon_{n_0}]_{i+1} &= \frac{U}{2}(n_0)(n_0+1) - E\sum_i e\cdot r_{i+1}(n_0+1) - \frac{U}{2}(n_0)(n_0-1) + E\sum_i e\cdot r_{i+1}(n_0) \\ &= Un_0 - E\sum_i e\cdot r_{i+1}\end{aligned} \tag{4.6}$$

So, the energy gap given, Eq.(2.9),

$$\Delta_0 = [\epsilon_{n_o-1} - \epsilon_{n_0}]_i + [\epsilon_{n_o+1} - \epsilon_{n_0}]_{i+1} = U - E \tag{4.7}$$

So, these dipole states differ in energy from the Mott state by

$$(U-E)$$

, so these states become degenerate at $U = E$ and an infinitesimal w leads to a resonant coupling between them. We need to identify the complete set of states resonantly coupled to the Mott state under these conditions, obtain the effective Hamiltonian within the subspace of these states, and determine its spectrum and correlations. The results will allow us to address the strong response of the Mott insulator to an electric field $E \approx U$ observed [2].

4.1 EFFECTIVE HAMILTONIAN IN ONE DIMENSION

In one spatial dimension, the set of all nearest-neighbor dipole states constitute the entire family of states resonantly coupled to the Mott insulator for $U = E$ and an infinitesimal w. Therefore, we introduce a new bosonic dipole creation operator, $d_l^\dagger$, to allow us to specify the resonant subspace and its effective Hamiltonian. Let $|Mn_0\rangle$ be the Mott insulator with n0 particles on every site. We identify this state with the dipole vacuum $|0\rangle$. Then the single dipole state is

$$d_l^\dagger|0\rangle \equiv \frac{1}{\sqrt{n_0(n_0+1}} b_l b_{l+1}^\dagger |Mn_0\rangle \tag{4.8}$$

with the constraints given as,

$$d_l^\dagger d_l \leq 1 \tag{4.9}$$

which refers to the fact that we cannot create more than one dipole resonantly on the same site, and also,

$$d_l^\dagger d_l d_{l+1}^\dagger d_{l+1} = 0 \tag{4.10}$$

which means that we cannot create two dipoles simultaneously on the nearest neighbor links, which will lead to a non-resonant state.

The effective Hamiltonian that would describe such a system of bosonic dipole operators,

$$H_d = -w\sqrt{n_0(n_0+1)}\sum_l (d_l + d_l^\dagger) + (U-E)\sum_l d_l^\dagger d_l \tag{4.11}$$

It costs energy $U-E$ to create each dipole, and each dipole can be created or annihilated with an amplitude of order w.

Now, to check if this H_d is the effective Hamiltonian and describes the same dynamics as the Hamiltonian in Eq.(4.1), we can check the dynamics of the bosonic creation operator, $d_l^\dagger$,

$$\begin{aligned}
[d_l^\dagger, H_d] &= [d_l^\dagger, -w\sqrt{n_0(n_0+1)}\sum_l (d_l + d_l^\dagger) + (U-E)\sum_l d_l^\dagger d_l] \\
&= [d_l^\dagger, -w\sqrt{n_0(n_0+1)}(d_l + d_l^\dagger) + (U-E) d_l^\dagger d_l] \\
&= -w\sqrt{n_0(n_0+1)} - (U-E) d_l^\dagger
\end{aligned} \tag{4.12}$$

Similarly,

$$\begin{aligned}
[d_l^\dagger, H] &= [d_l^\dagger, -w\sum_{<i,j>}(b_i^\dagger b_j + b_j^\dagger b_i) + \frac{U}{2}\sum_i n_i(n_i-1) - E\sum_i e\cdot r_i n_i] \\
&= [d_l^\dagger, -w\sqrt{n_0(n_0+1)}\sum_l (d_l + d_l^\dagger)] \\
&\quad + [d_l^\dagger, \frac{U}{2}(b_l^\dagger b_l b_l^\dagger b_l - b_l^\dagger b_l + b_{l+1}^\dagger b_{l+1} b_{l+1}^\dagger b_{l+1} - b_{l+1}^\dagger b_{l+1})] \\
&\quad + [d_l^\dagger, -E r_l b_l^\dagger b_l - E r_{l+1} b_{l+1}^\dagger b_{l+1}] \\
&= -w\sqrt{n_0(n_0+1)} - U d_l^\dagger + E d_l^\dagger \\
&= -w\sqrt{n_0(n_0+1)} - (U-E) d_l^\dagger
\end{aligned} \tag{4.13}$$

Therefore, the effective Hamiltonian, H_d, correctly describes the dynamics of the original Hamiltonian in Eq.(4.1).

Also, the Hamiltonian, H_d, and the constraints (4.9, 4.10) can also be written in the form of a quantum spin chain. We can write the dipole present/absent configuration on a site l as a pseudospin σ_l^z up/down where $\sigma^{x,y,z}$ represents the Pauli matrices.

Then $\sigma_l^z = 2d_l^\dagger d_l - 1$ and $\sigma_l^x = d_l^\dagger + d_l$, hence

$$H_d = \sum_l \left[-w\sqrt{n_o(n_0+1)}\sigma_l^x + (U-E)(\sigma_l^z+1)/2 + J(\sigma_l^z+1)(\sigma_{l+1}^z+1)\right] \tag{4.14}$$

The constraint (4.9) is implemented by taking $J \to \infty$ limit of the last term. Now, as we find the phase transition conditions for H_d, we would see amazing resemblances to that of the Ising Model for spin 1/2 chain.

4.2 DIAGONALIZING THE DIPOLE HAMILTONIAN

The eigenstates of H_d are characterized by n_0 and the single dimensionless number

$$\lambda = \frac{U - E}{w} \tag{4.15}$$

Before we numerically analyze the spectra, let's think about the extreme cases of λ.

When λ becomes very large ($\lambda \to \infty$), it implies that the energy difference $U - E$ between creating a dipole and the effect of the external electric field is significantly larger than the characteristic hopping energy w. In this limit, the hopping term becomes relatively less important compared to the energy cost of creating dipoles.

In the ground state, the system tends to minimize its energy. Since creating dipoles is energetically costly, the ground state wavefunction will seek to minimize the number of dipoles present. This means that the dipoles will be strongly suppressed, and the system will tend to resemble the Mott insulator state, where each site has a fixed number of particles (n_0 particles) and dipoles are not favoured due to their energy cost and the ground state wavefunction will approximate the Mott insulator state $|Mn_0\rangle$, which corresponds to the case where no dipoles are created.

This behavior is consistent with the expectation that as the energy difference between the Mott state and the external field becomes very large, the system will try to minimize any fluctuations that cost energy, which in this case corresponds to suppressing the creation of dipoles.

On the other hand, the opposite limit $\lambda \to -\infty$, the ground state is doubly degenerate, because there are two distinct states with maximal dipole number: $(d_1^\dagger, d_3^\dagger, d_5^\dagger \cdots)|0\rangle$ and $(d_2^\dagger, d_4^\dagger, d_6^\dagger \cdots)|0\rangle$.

This immediately suggests the existence of an Ising quantum critical point at some intermediate value of λ, associated with an order parameter which is a density wave of dipoles of period two lattice spacings.

Let's diagonalize the Hamiltonian H_d numerically.

To diagonalize it, we identify the dipole creation operator, which acts on the Mott-state to create a one-dipole state,

$$d_l^\dagger|0\rangle = \begin{bmatrix} \vdots & \\ -1 & (l^{th} \text{ site}) \\ +1 & ((l+1)^{th} \text{ site}) \\ 0 & \\ \vdots & \end{bmatrix} \begin{bmatrix} \vdots \\ n_0 \\ n_0 \\ n_0 \\ \vdots \end{bmatrix} = \begin{bmatrix} \vdots & \\ n_0 - 1 & (l^{th} \text{ site}) \\ n_0 + 1 & ((l+1)^{th} \text{ site}) \\ n_0 & \\ \vdots & \end{bmatrix} \tag{4.16}$$

Also, we need to take care of the periodic boundary conditions. For N=8, we found 47 dipole states that are resonant with the energy $U - E$. (1: Mott state, 8: 1-dipole state, 20: 2-dipole state, 16: 3-dipole states and 2: 4-dipole states or maximal dipole states).

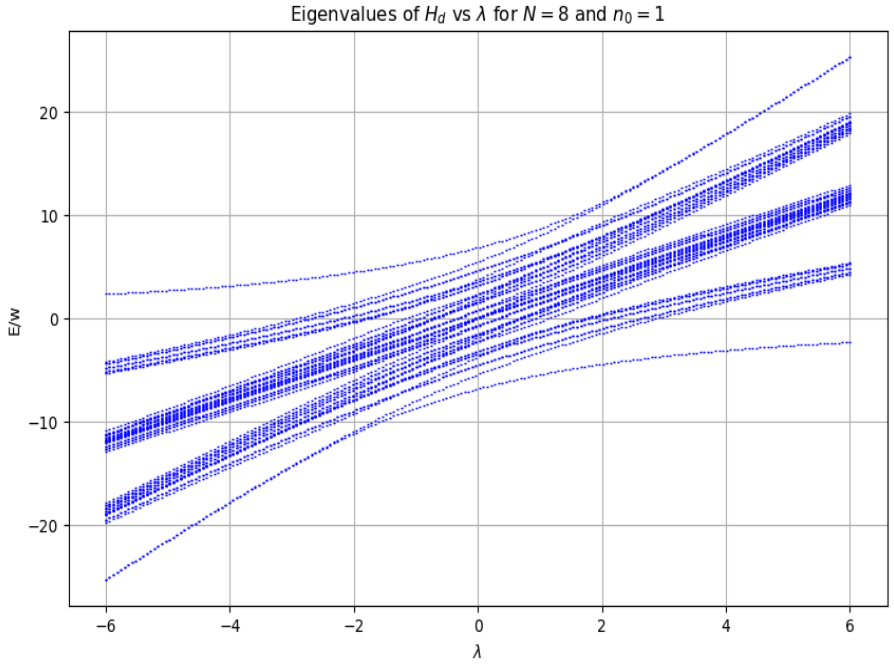

Figure 4.1: All the eigenvalues of H_d for $N = 8$ and $n_0 = 1$.Note that the ground state is non-degenerate for positive λ,and there are two low-lying levels with an exponentially small splitting for $\lambda < 0$ and $|\lambda|$ large

Fig.(4.1) shows a unique ground state for $\lambda \to \infty$ and a two-fold degenerate state for $\lambda \to -\infty$. Above these lowest energy states, there is a finite energy gap, and the excited states have clearly split into bands corresponding to the various "particle" continua; these "particles" are dipoles for $\lambda \to \infty$, and domain-walls between the two ground states for $\lambda \to -\infty$.

To test for the quantum critical point at the intermediate points of λ, we plot the energy gap Δ of the lowest two of the eigenvalues plotted in Fig.(4.1). In regions of negative λ, the system tends towards two degenerate ground states, causing the energy gap Δ to diminish exponentially as the system size N increases. Conversely, for positive λ values, Δ converges to a finite non-zero value, specifically $U - E$. If these two phases are separated by a quantum critical point, then we can identify a quantum critical point λ_c where a phase transition occurs. At this critical point, the energy gap is anticipated to scale as $\Delta \approx N^{-z}$, with the dynamic critical exponent z serving as a crucial parameter characterizing the transition. To observe this, we plot $N\Delta$ as a function of λ in Fig.(4.2). A distinctive crossing point emerges at $\lambda_c \approx -1.850$, a clear indicator of the Ising quantum phase transition($z = 1$). Interestingly, this critical point deviates from the expected value $E = U$ at $\lambda = 0$. The observed crossing point at $\lambda_c \approx -1.850$ is interpreted as the manifestation of the Ising quantum critical point. The deviation of the

critical point from the expected value $E = U$ highlights the significant influence of quantum fluctuations on the system's behavior.

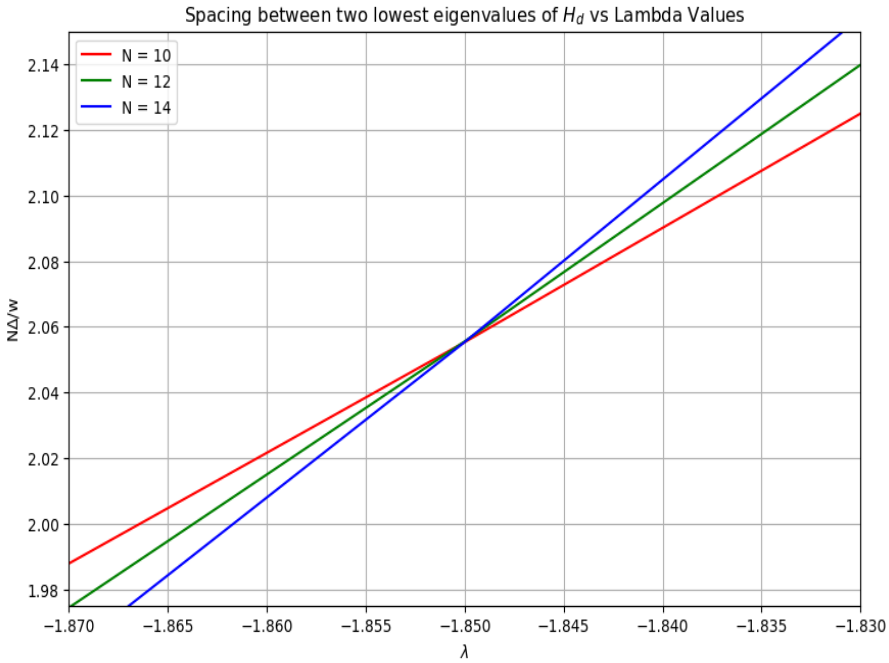

Figure 4.2: The spacing between the lowest two eigenvalues of $H_d(= \Delta)$ as a function λ for various system sizes and $n_0 = 1$.We used periodic boundary conditions for H_d.

Another test for the Ising criticality is given by rescaling the horizontal axis of Fig.(4.2) with N. The test discussed involves examining the scaling behavior of the energy gap (Δ) in the system obeying the scaling form,

$$\Delta = N^{-z}\phi(N^{1/v}(\lambda - \lambda_c)) \tag{4.17}$$

where ϕ is a universal scaling function, and v is the correlation length exponent. We test for Eq.(4.17) in Fig.(4.3) with the Ising exponent $v = 1$.

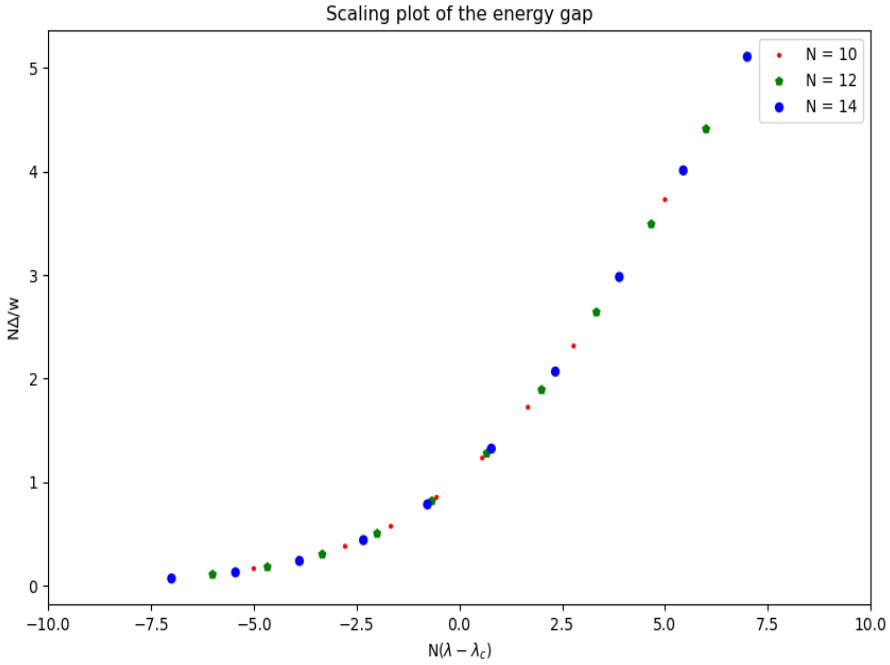

Figure 4.3: Scaling plot of the energy gap to test for (4.17). We used $\lambda_c = 1.850$ and $n_0 = 1$.

4.3 FEDILITY SUSCEPTIBILITY

The position of a generic continuous critical point is indicated by the peak of the fidelity susceptibility, which is defined as the derivative of fidelity with respect to the small shift of the external parameter. We see that in the BHM transition the value of the external parameter for which the system is changing most rapidly, manifested by the universal peak in fidelity susceptibility, is significantly shifted from the critical point toward the gapped phase[3] .

In Fig. 4.4, we show the fidelity susceptibility for the BHM at fillings n = 1 for systems with lattice sites, N= 10, 12, 14 and for on-site interactions U = 1. χ exhibits clear maxima for values of U greater than U_c computed from the scaling of the gap. Consistent with the results in [3], the maxima positions are seen to move toward weaker interactions and their height increases with increasing system size.

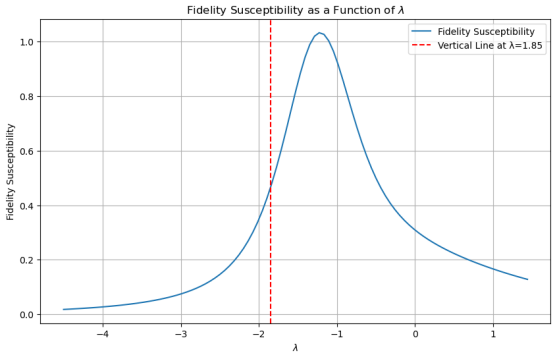

(a) N=10

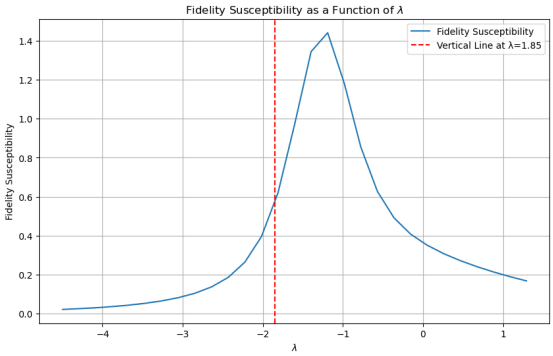

(b) N=12

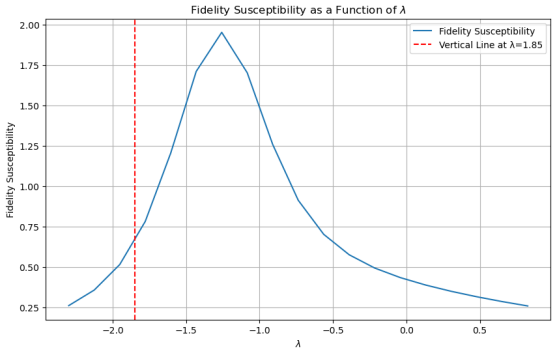

(c) N=14

Figure 4.4: Fidelity susceptibility for different system sizes at integer filling $n_0 = 1$

As we can see that the point at which Fidelity Susceptibility is maximum, is shifted to the right. But, as the size of the system increases, it shifts to the left towards the original critical point and in the thermodynamical limit, it will be equal to the actual critical point[5].

5 Cavity Quantum Electrodynamics

Cavity Quantum Electrodynamics (CQED) investigates the interaction of light and atoms/molecules in the regime where a single photon significantly modifies the radiative properties of the scattering particles. These conditions are achieved by using a high-finesse resonator, which acts as an effective trap for photons, thereby increasing the interaction strength between a single photon and a single atom. The technology of experiments with optical and microwave cavities has reached a level of control, that has led to the observation of predictions at the core of quantum mechanics as well as the realization of basic elements of quantum information processing. These results follow theoretical models, which have been developed few decades ago and which provide a reliable theoretical framework for the description of the dynamics of these systems.

5.1 COHERENT DYNAMICS OF AN ATOM COUPLED TO A CAVITY FIELD

In CQED, a single atom interacts with a single mode of a high-finesse optical cavity. The atom is modeled as a two-level system with a ground state $|1\rangle$ and an excited state $|2\rangle$, separated by the transition frequency ω_0. The atomic Hamiltonian is given by:

$$\hat{H}_{at} = \hbar\omega_0\hat{\sigma}^\dagger\hat{\sigma} \tag{5.1}$$

where $\hat{\sigma} = |1\rangle\langle 2|$ and $\hat{\sigma}^\dagger = |2\rangle\langle 1|$ are the lowering and raising operators, respectively.

Next, we consider an optical cavity constituted by two reflecting mirrors separated by the linear distance L. The boundary conditions at the mirrors of the cavity impose a discrete spectrum of field modes along the cavity axis, such that the mode frequencies are equi-spaced and at distance $\Delta w = 2\pi c/L$, with c the speed of light in the vacuum. an atomic transition at frequency w_0 can be close to the frequency of one cavity mode, say at frequency w_c, and very far-detuned from other modes. In this limit one can talk of a "single- mode" cavity.

The cavity mode, with frequency ω_c, is described by the annihilation and creation operators $\hat{a}$ and $\hat{a}^\dagger$, with the cavity Hamiltonian:

$$\hat{H}_C = \hbar\omega_c\left(\hat{a}^\dagger\hat{a} + \frac{1}{2}\right) \tag{5.2}$$

Let us assume that the dipolar transition $|1\rangle \rightarrow |2\rangle$ at a position($\hat{r}$) couples quasi-resonantly with the mode c of the resonator. Under the assumption that only one cavity mode interacts

resonantly with the atomic transition, the atom-cavity interaction, in the electric-dipole approximation and after applying the rotating-wave approximation, is given by the Jaynes-Cummings Hamiltonian:

$$\hat{H}_{int} = \hbar g(\hat{\mathbf{r}})(\hat{\sigma}^\dagger \hat{a} + \hat{a}^\dagger \hat{\sigma}) \tag{5.3}$$

Here, $g(\hat{\mathbf{r}})$ is the position-dependent vacuum Rabi frequency, which determines the atom-cavity coupling strength.

The Hamiltonian governing the coupled dynamics of a single atom and a single cavity mode is given by the Jaynes-Cummings Hamiltonian:

$$\hat{H}_{JC} = \hbar\omega_0 \hat{\sigma}^\dagger \hat{\sigma} + \hbar\omega_c \hat{a}^\dagger \hat{a} + \hbar g(\hat{r})(\hat{\sigma}^\dagger \hat{a} + \hat{a}^\dagger \hat{\sigma}) \tag{5.4}$$

Here, ω_0 is the atomic transition frequency, $\hat{\sigma}$ and $\hat{\sigma}^\dagger$ are the lowering and raising operators for the atom, ω_c is the cavity mode frequency, $\hat{a}$ and $\hat{a}^\dagger$ are the annihilation and creation operators for the cavity mode, and $g(\hat{r})$ is the vacuum Rabi frequency, which depends on the atom-cavity coupling strength.

The dynamics of the closed atom-cavity system is governed by the Schrödinger equation:

$$i\hbar \frac{\partial |\Psi(t)\rangle}{\partial t} = \hat{H}_{tot} |\Psi(t)\rangle \tag{5.5}$$

where $|\Psi(t)\rangle$ is the quantum state of the system at time t. The time evolution of the quantum state describes various phenomena, such as vacuum Rabi oscillations, cavity cooling, and the generation of non-classical states of light.

5.2 EXTERNAL PUMP: LASER DRIVING THE ATOMS

Energy is typically pumped into the atom-cavity system by injecting photons into the cavity field or by driving the atomic transition with an external laser field. The Hamiltonian describes the interaction between the laser and the atom:

$$\hat{H}_L = i\hbar\Omega(\hat{\sigma}^\dagger e^{i(\mathbf{k}_p \cdot \hat{\mathbf{r}} - \omega_p t)} - \hat{\sigma} e^{-i(\mathbf{k}_p \cdot \hat{\mathbf{r}} - \omega_p t)}) \tag{5.6}$$

Here, Ω is the Rabi frequency determining the laser-atom coupling strength, $\mathbf{k}_p$ is the laser wave vector, ω_p is the laser frequency, and $\hat{\mathbf{r}}$ is the position operator of the atom. The total Hamiltonian for the system is the sum of the external, Jaynes-Cummings, and laser Hamiltonians: $\hat{H}_{tot} = \hat{H}_{ext} + \hat{H}_{JC} + \hat{H}_L$.

6 Two-Site Bose Hubbard Model in a Cavity

A method to investigate the superfluid-insulator transition of cold atoms in optical lattices using the transmission spectra of an optical cavity is of great excitement. The atoms interact with a quantised cavity mode in a dispersive manner, effectively behaving as moving refractive media within the cavity. The transmission spectra of the cavity directly reflect the quantum or classical distributions of the atoms, distinguishing between the superfluid and insulator phases. This non-destructive technique capitalizes on the strong coupling regime, where even a single atom can induce a significant shift in the cavity resonance.

Atoms are trapped in a double-well potential and interact dispersively with a damped and driven field mode. To gain insight into the dynamics of the system, we assume the system starts from an initial state and evolves towards the steady state.

We assume N two-level bosonic atoms, transition frequency w_a are trapped in a double well potential V(x) and loaded in an optical cavity, where they interact with a cavity field mode with frequency w_c. The cavity is excited by a weak laser of frequency ω_p and amplitude η through the mirror. We assume that the detuning between the atom and the field greatly exceeds the atomic spontaneous emission rate and the Rabi frequency, allowing us to adiabatically eliminate the atomic upper level, thereby neglecting the atomic internal dynamics.

After adiabatic elimination, the Hamiltonian for a single atom plus the field in the frame rotating at the frequency of the pumping field can be expressed as:

$$H_0 = H_{ph} + H_s$$

where H_{ph} is the Hamiltonian in the rotating frame for the driven field:

$$H_{ph} = -\Delta a^\dagger a + \eta(a + a^\dagger)$$

Here, $\Delta = \omega_p - \omega_c$ represents the detuning between the pump and cavity frequencies.

The term H_s represents the Hamiltonian for a single atom in the superposition of a classical potential $V(x)$ and a quantum potential $u^2(x)U_0 a^\dagger a$:

$$H_s = \frac{p^2}{2m} + V(x) + u^2(x)(U_0 a^\dagger a)$$

Here, $u(x)$ is the field mode function normalized to unity at the antinode, and $U_0 = \frac{g_0^2}{\omega_c - \omega_a}$, where g_0 represents the atom-field coupling at the antinode.

Assuming that wannier function does not change with interaction for this simpler case, we can also write the atomic Hamiltonian.

The Hamiltonian for the atomic subsystem is denoted as H_a and is given by:

$$H_a = -t(b_1^\dagger b_2 + b_2^\dagger b_1) + u[(n_1(n_1-1) + n_2(n_2-1))] + \epsilon(n1 - n2)$$

Here, we introduce the atom number operators $n_i = b_i^\dagger b_i$ (for $i = 1, 2$). ϵ is the tilt parameter. The atomic tunneling rate t and the on-site interaction energy u are defined as:

$$-t = \int d^3x w_1^*(x)(-\frac{\nabla^2}{2m} + V(x))w_2(x)$$

$$u = \frac{4\pi a_s}{m}\int d^3x |w_{1,2}(x)|^4$$

The interaction between the atoms and the field, denoted as H_{int}, is described by:

$$H_{int} = \int d^3x \Psi^\dagger(x)u^2(x)\Psi(x)(U_0 a^\dagger a) \approx (J_1 n_1 + J_2 n_2)(U_0 a^\dagger a)$$

Here, the dimensionless coefficients J_1 and J_2 are defined as:

$$J_{1,2} = \int d^3x u^2(x)|w_{1,2}(x)|^2$$

These coefficients reflect the overlap between the atomic modes and the field mode, with $0 \leq J_{1,2} \leq 1$ due to the normalization conditions of $u(x)$ and $w_{1,2}(x)$. In the case where $J_1 = J_2$, the dynamics of the atoms and the field are decoupled. We focus on the case where $J_1 \neq J_2$, assuming $J_1 = 1$ and $J_2 = 0$ without loss of generality. This allows us to define effective parameters $\Delta' = \Delta - U_0 J_2 N$ and $U_0' = U_0(J_1 - J_2)$, leading to the Hamiltonian:

$$H = -t(b_1^\dagger b_2 + b_2^\dagger b_1) + u(n_1(n_1-1) + n_2(n_2-1)) + \epsilon(n1-n2) + U_0' a^\dagger a n_1 - \Delta' a^\dagger a + \eta(a + a^\dagger) \tag{6.1}$$

This effectively simplifies the interaction terms to $J_1 = 1$ and $J_2 = 0$.

It is always easier to do this numerical analysis in Qutip, so for easier representation in Qutip, we should also convert this into a spin system,

$$H = -tS_x + u\frac{S_z^2 + N^2}{2 - N} + \epsilon S_z + U_0' a^\dagger a \frac{S_z + N}{2} + \Delta' a^\dagger a + \eta(a + a^\dagger) \tag{6.2}$$

The Hamiltonian derived above controls the coherent evolution of the atom-field system. However, we still have to take the dissipation into account, which comes from the cavity loss in the model we consider. The evolution of the system is described by the master equation:

$$\dot{\rho} = -i[H, \rho] + \kappa(2a\rho a^\dagger - a^\dagger a\rho - \rho a^\dagger a) \equiv \mathcal{L}\rho$$

Here, ρ represents the density matrix of the atom-field system in the rotating frame, and κ is the cavity loss rate.

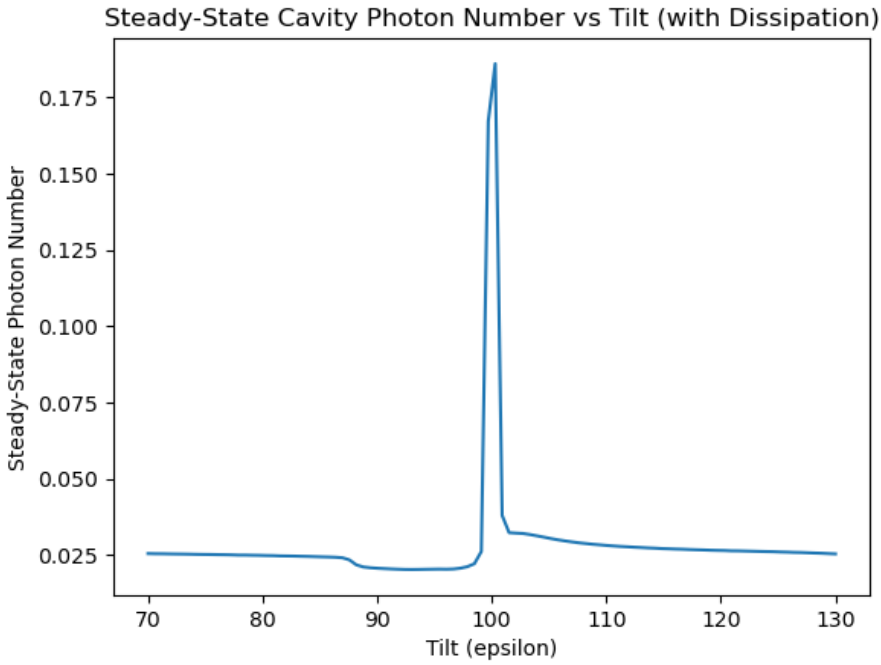

Figure 6.1: Steady State Cavity Photon Number Vs Tilt

The photon number suddenly increases at $\epsilon = 102$, which is close to U, indicating that we can use this as a measure of Quantum Phase Transition. As we have seen before, in the double-well system, the transition point was at $U = \epsilon$. The steady-state photon number is a good indicator of the critical point.

And understanding the fidelity susceptibility might also give us a better understanding of detecting the critical point,

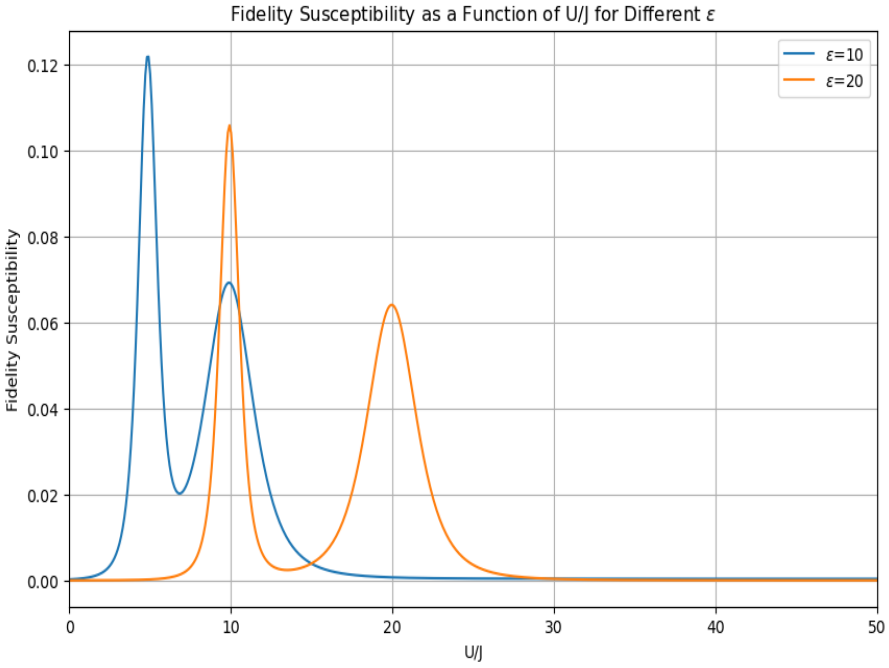

Figure 6.2: Fidelity Susceptibility as a Function of U/J for Different ϵ

The fidelity susceptibility shows two peaks, one at $U = \epsilon/2$ and $U = \epsilon$, this is because the cavity photon also reaches a maxima twice, a smaller one at $\epsilon/2$ and bigger one at ϵ. We need to understand why the cavity photon number is resonant at these two points.

7 Conclusion

In this thesis, we delved into the Quantum Phase Transition of a closed system, particularly investigating the behavior of the two-site Bose Hubbard Model (BHM) concerning tilt-induced critical points. We found that these critical points remain constant irrespective of system size, although the phase transition becomes more pronounced in larger systems. Our analysis heavily relied on studying the fidelity susceptibility, which showed an increasing trend with system size while maintaining a consistent critical point location. Additionally, we identified that the critical point for the two-site BHM aligns with the resonance of U. Transitioning to the cavity setup, we observed that the critical point could also be discerned by examining the steady-state photon number within the cavity.

Expanding our scope, we explored the extended full BHM and observed how introducing a tilt shifts the critical point, presenting a potential sensor signal. Interestingly, the fidelity susceptibility, initially maximum and shifted rightward, tends to move leftward towards the original critical point as the system size increases, eventually converging to the actual critical point in the thermodynamic limit.

Looking ahead, our focus shifts to investigating the behavior of the entire extended tilted BHM within a cavity, aiming to analyze the steady state and fidelity susceptibility. By tuning the critical point, akin to the tiled 2-site model, we envision using this setup as a force sensor finely tuned to the critical point of the phase transition.

Bibliography

[1] M. P. A. Fisher, P. B. Weichman, G. Grinstein and D. S. Fisher. 1989. Boson localization and the superfluid-insulator transition. *Physical Review B*. DOI: 10.1103/PhysRevB.40.546 (cit. on p. 12).

[2] M. Greiner, O. Mandel, T. Esslinger, T. W. Hänsch and I. Bloch. 2002. Quantum phase transition from a superfluid to a Mott insulator in a gas of ultracold atoms. *Nature 415*. DOI: 10.1038/415039a (cit. on pp. 12, 24, 25).

[3] M. R. Juan Carrasquilla Salvatore R. Manmana. 2013. Scaling of the gap, fidelity susceptibility, and Bloch oscillations across the superfluid to Mott insulator transition in the one-dimensional Bose-Hubbard model. *Phys. Rev. A 87, 043606*. DOI: doi.org/10.1103/PhysRevA.87.043606 (cit. on p. 30).

[4] J. Larson, S. Fernández-Vidal, G. Morigi and M. Lewenstein. 2008. Quantum stability of Mott-insulator states of ultracold atoms in optical resonators. *New Journal of Physics*, 10, (Apr. 2008), 045002, 4, (Apr. 2008). DOI: 10.1088/1367-2630/10/4/045002 (cit. on p. 3).

[5] A. V. P. Buonsante. 2007. Ground-State Fidelity and Bipartite Entanglement in the Bose-Hubbard Model. *Phys. Rev. Lett. 98, 110601*. DOI: 10.1103/PhysRevLett.98.110601 (cit. on p. 31).

[6] C. J. Pethick and H. Smith. 2008. Bose–Einstein Condensation in Dilute Gases. *Cambridge University Press* (cit. on pp. 14, 15).

[7] M. K. O. R Gati. 2007. A bosonic Josephson junction. *Journal of Physics B*. DOI: 10.1088/0953-4075/40/10/R01 (cit. on p. 20).

[8] S. Sachdev. 2011. Quantum Phase Transitions. *Cambridge University Press* (cit. on p. 13).

[9] S. Sachdev, K. Sengupta and S. M. Girvin. 2002. Mott insulators in strong electric fields. *Physical Review B*, 66, (Aug. 2002), 075128, 7, (Aug. 2002). DOI: 10.1103/PhysRevB.66.075128 (cit. on pp. 3, 24).

[10] H. Stoof, D. Dickerscheid and K. Gubbels. 2014. Ultracold Quantum Fields. Theoretical and Mathematical Physics. *Springer Netherlands* (cit. on p. 16).